Ship Observations of the Tropical Pacific Ocean along the Coast of South America

S. P. DE SZOEKE, C. W. FAIRALL, AND SERGIO PEZOA

NOAA/Earth System Research Laboratory/Physical Sciences Division, Boulder, Colorado

ABSTRACT

In October 2007 the NOAA ship *Ronald H. Brown* sailed southward within 300 km of the coast of Ecuador and Peru, sampling surface meteorology, air–sea turbulent and radiative fluxes, cloud properties, and upper-air soundings from the equator to 20°S. Two distinct water masses characterize the coastal region: cold-pool water below 19°C in the Southern Hemisphere, and warm-pool water above 20°C to the north, with a transition between the water masses at 2.5°S. Net turbulent and radiative fluxes warm the cool water south of 2.5°S by 100 W m^{-2} but do not warm the equatorial water significantly. Winds blow parallel to the shore, about 5 m s^{-1} over the cold pool and 7 m s^{-1} over the equator. Stratocumulus clouds are remarkably solid over the coastal cold pool, with only brief periods of partial clearing, mostly in the afternoon. Lower aerosol concentrations and thicker clouds observed farther from the coast on 22–23 October are coincident with a pocket of open cells seen to the west and southwest of the ship. Observations from this cruise and other NOAA Stratus cruises (2001 and 2003–07) are suitable for comparison with model simulations and provide context for future field experiments. These datasets are publicly available.

1. Introduction

The temperature of the tropical Pacific Ocean at the coastal boundary is determined by a complex balance of upwelling, surface fluxes, and transport, which in turn depend on the wind and solar forcing at the ocean surface. Southeasterly winds blow parallel to the coast in the Southern Hemisphere, causing offshore Ekman transport and coastal upwelling that cools the ocean surface. Coastal sea surface temperature (SST) anomalies propagate westward by Bjerknes (1969) and wind–evaporation–SST feedback (reviewed by Xie 2004). SST anomalies are amplified by the positive feedback of high-albedo stratus clouds that form over cold water in the marine atmospheric boundary layer (MABL). Thus coastal SST is important for the whole ocean: cool SST along the Southern Hemisphere coast of South America initiates the meridional asymmetry of heating and the corresponding asymmetric atmospheric Hadley circulation over the Pacific Ocean. The asymmetry resulting from coupled coastal processes has consequences for the seasonal cycle of the tropical Pacific

and migration of the intertropical convergence zone (Xie 1994; de Szoeke and Xie 2008).

Because of the shallow MABL, steep Andean mountains, and coupled cloud, aerosol, and ocean interactions, simulating stratiform clouds and surface winds has been challenging for coupled regional and global general circulation models (Ma et al. 1996; Gordon et al. 2000). These interactions are the focus of the Variability of American Monsoon Systems (VAMOS) Ocean Cloud Atmosphere Land Study (VOCALS) regional experiment planned for autumn 2008. Already Stratus cruises undertaken jointly by the National Oceanic and Atmospheric Administration (NOAA) and Woods Hole Oceanographic Institution (WHOI) in autumn of 2001 and 2003–07 have ventured into the southeastern tropical Pacific to quantify the ocean, MABL, and cloud dynamics responsible for the near-surface heat budget. In 1999, the research cruise CIMAR-5 traversed from the Chilean coast to Easter Island (110°W) along 27°S (Garreaud et al. 2001). Marine stratocumulus clouds have previously been observed during the Tropical East Pacific Process Studies (TEPPS) cruise over the northeast subtropical Pacific (Yuter et al. 2000) and in the Atlantic during the Atlantic stratocumulus transition experiment (ASTEX; Albrecht et al. 1995).

In collaboration with Ecuadorian and Peruvian sci-

Corresponding author address: S. P. de Szoeke, NOAA/ESRL/ Physical Sciences Division, 325 Broadway, R/PSD3, Boulder, CO 80305.
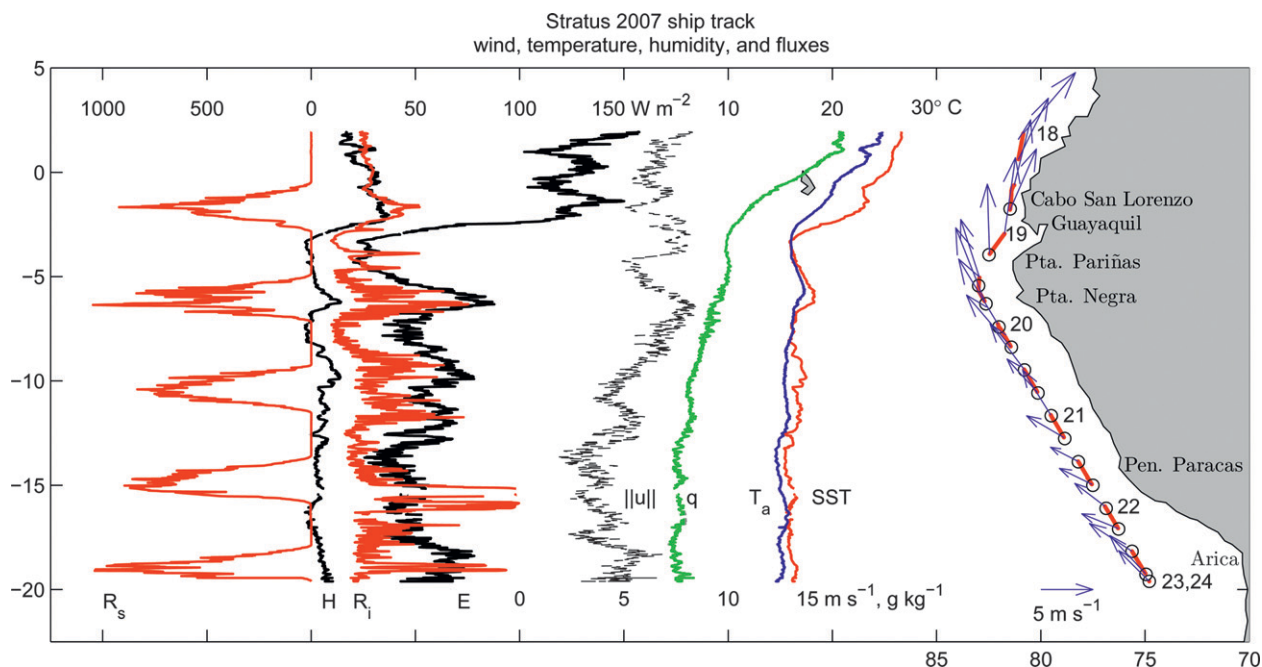E-mail: simon.deszoeke@noaa.gov

FIG. 1. Track of the *RHB* along the coast of South America on the 2007 Stratus cruise. Dashed red lines indicate 6-h intervals; days 18–24 October are printed at right. 6-h average observed surface wind vectors (blue) point from the ship track. Curves from right to left of ship track: SST (T_s, red), 18-m air temperature (T_a, blue) and humidity (q, green), surface turbulent latent and sensible (H and E, black), and net radiative solar and thermal infrared (R_s and R_i, red) fluxes.

entists and their governments, the NOAA/WHOI Stratus cruise in October 2007 made a unique transect along the coast of South America, from the equator to 20°S within 300 km of shore. The track of the ship on this transect is shown by the dashed line following the coast at right in Fig. 1. Each red dash is a 6-h interval, and numbers along the track indicate the date of October, coordinated universal time (UTC). The ship traveled into the wind from north to south.

During the period of this coastal leg (18–23 October), SST is anomalously negative south of the equator compared to climatology. The anomaly is more than −2°C south of Guayaquil, and reaches −3°C along the central coast of Peru. This corresponds to a broad 1-hPa high pressure anomaly off the coast of Peru. Local wind anomalies do not appear to force the SST pattern, but diverge over the high pressure anomaly.

2. Instruments and sampling

Three sets of instruments on the NOAA ship *Ronald H. Brown* (*RHB*) made measurements during the 2007 Stratus cruise (Fairall et al. 2003; Fairall and Bradely 2006): NOAA Physical Science Division (PSD) near-surface meteorology, cloud remote sensing and aerosol number sampling from the ship, and upper-air soundings. The NOAA PSD Weather and Climate Physics

Branch [formerly the Environmental Technology Laboratory (ETL)] has outfitted the *RHB* with a mobile set of accurate and fast sensors that acquire observations of the near-surface atmosphere with an accuracy suitable to compute air–sea fluxes (Fairall et al. 2003). Instruments on a jackstaff at the bow of the ship sample air temperature, humidity, wind, and ship motion. Sea surface temperature is measured by a floating "sea snake" thermometer at approximately 5-cm depth. At this depth the thermometer samples the daylight warm layer, but not the cool skin layer. The optical rain gauge malfunctioned and was switched off during Stratus 2007.

Turbulent fluxes of momentum, heat, and humidity presented here are computed by the Fairall et al. (2003) algorithm from bulk quantities measured by instruments on a jackstaff at the bow of the ship. The bulk fluxes compare well with available fluxes computed by covariances of high-rate (20 Hz) temperature and velocity components from a sonic anemometer–thermometer. High-rate observations of water vapor were made by a 3-band infrared Licor 7500 optical absorption instrument. The 2007 Stratus cruise pioneered the use of multiple Licor instruments, with the goal of developing a reliable autonomous shipboard system with enough precision to measure CO_2 fluxes directly. Downward solar and thermal infrared radiation are measured by a

pyranometer and a pyrgeometer, respectively. Surface meteorology and fluxes were averaged to standard 5-min time intervals beginning on the hour.

NOAA PSD uses an upward-looking Radiometrics "mailbox" 20.6- and 31.65-GHz channel passive microwave radiometer to estimate column water vapor and liquid water (Fairall et al. 2008). Liquid water paths are physically retrieved following Zuidema et al. (2005). Although instrument calibrations are not always well known, the retrieved liquid water paths typically compare well to sonde-calculated values. A Vaisala 905-nm lidar ceilometer estimates cloudiness and up to 3 cloud-base heights. An active 915-MHz NOAA radar wind profiler was operated with its antenna pointed vertically. Turbulence and gradients of temperature and humidity at the MABL inversion scatter the radar pulse, from which we diagnose the height of the boundary layer to the nearest 60-m range gate. Valid returns from these three sensors are averaged to standard 5-min intervals.

Vaisala global positioning system (GPS) digital rawinsondes were released into the atmosphere from the fantail of the ship approximately every 6 h during the coastal transect from 18 to 23 October. The rawinsonde release times and locations are indicated by open circles along the ship track in Fig. 1. Rawinsondes measured and telemetered temperature, relative humidity, pressure, and GPS position. Profiles of temperature, humidity, and winds with height are calculated and averaged to standard 10-m altitudes.

3. Surface meteorology

Arrows originating from the dashed ship track in Fig. 1 are centered 6-h averages of the surface wind. The wind was extremely constant within each 6-h period, with speed standard deviation less than or equal to 1 m s^{-1}. The wind speed $|\mathbf{u}|$ (black dashed line) is on average 5.6 m s^{-1}, with a 0.4 m s^{-1} offshore component. The wind follows the contour of the coast with a standard deviation in direction of under 20° in any 6-h period. South of 12°S winds are as much as 40° offshore of parallel to the local coast, perhaps reflecting the heading of the coast upstream of the ship between Paracas Peninsula and Arica, or the influence of high surface pressure found over cool coastal SST and over subtropical latitudes.

The SST (red) and air temperature (blue) are plotted to the left of the ship track in Fig. 1. SST reaches a minimum of 15.5°C at 14°S and a maximum of 26.6°C at 2°N. Air temperature follows SST. The sea–air temperature difference is about 1.3°C south of 3°S, with diurnal variations of the same magnitude. On the nights

TABLE 1. Heat flux components (W m^{-2}) into the ocean for the coastal transect, north of 2.5°S and south of 2.5°S.

	Whole track	Lat > 2.5°S	Lat < 2.5°S
Solar	188	(147)	(198)
IR	−30	−30	−30
Sensible	−8	−27	−4
Latent	−66	−125	−52
Total	82	6	102

of 18, 19, and 21 October (local time) the SST cooled off to equal the air temperature, occasionally resulting in sensible heat flux from the air to the ocean. The air temperature is considerably cooler than the SST (3.5°C) in the warm pool north of 3°S, because advection from the south has a cooling effect of approximately 10°C day^{-1} on the surface air. The largest sea–air temperature difference of 4.25°C was observed in the afternoon and downstream of the strong gradient at 2.5°S.

At left in Fig. 1 is the profile of air–sea heat fluxes along the track. Positive (rightward) fluxes represent heat leaving the ocean. The red curves are solar (R_s) and thermal infrared (R_i) fluxes. The solar flux is plotted on a scale one tenth of the scale of the other fluxes, and its pulses indicate the time of local daylight. The black curves are latent and sensible turbulent heat fluxes. Latent heat flux E is in the neighborhood of 100–150 W m^{-2} north of 2.5°S, and about 50 W m^{-2} south of 2.5°S. Sensible heat flux H is about 30 and 10 W m^{-2} north and south of 2.5°S. Though solar flux has large diurnal variations, it does not appear to be noticeably different either side of 2.5°S. The variability of the infrared flux increases south of 2.5°S, probably because the atmosphere has less water vapor and downward thermal radiation is more strongly modulated by clouds. Table 1 shows a mean heat budget of the upper ocean, averaging the whole coastal ship track, the part north of 2.5°S, and the part south of 2.5°S. To avoid diurnal sampling biases, we use the solar radiation averaged over the whole coastal leg for all of the budgets. The average solar radiation for the partial legs is nevertheless indicated in parentheses. In the warm pool to the north, the ocean surface is not losing or gaining heat within measurement error. Yet on the southern part of the leg, the cool ocean is warmed by a net 100 W m^{-2}.

4. Clouds and upper-air soundings

Rawinsondes were launched from the ship every 6 h beginning 1800 UTC 18 October and every 4 h on 23 October, providing snapshots of the vertical temperature and humidity structure of the atmosphere. All the soundings on the coastal leg are compiled in a time–
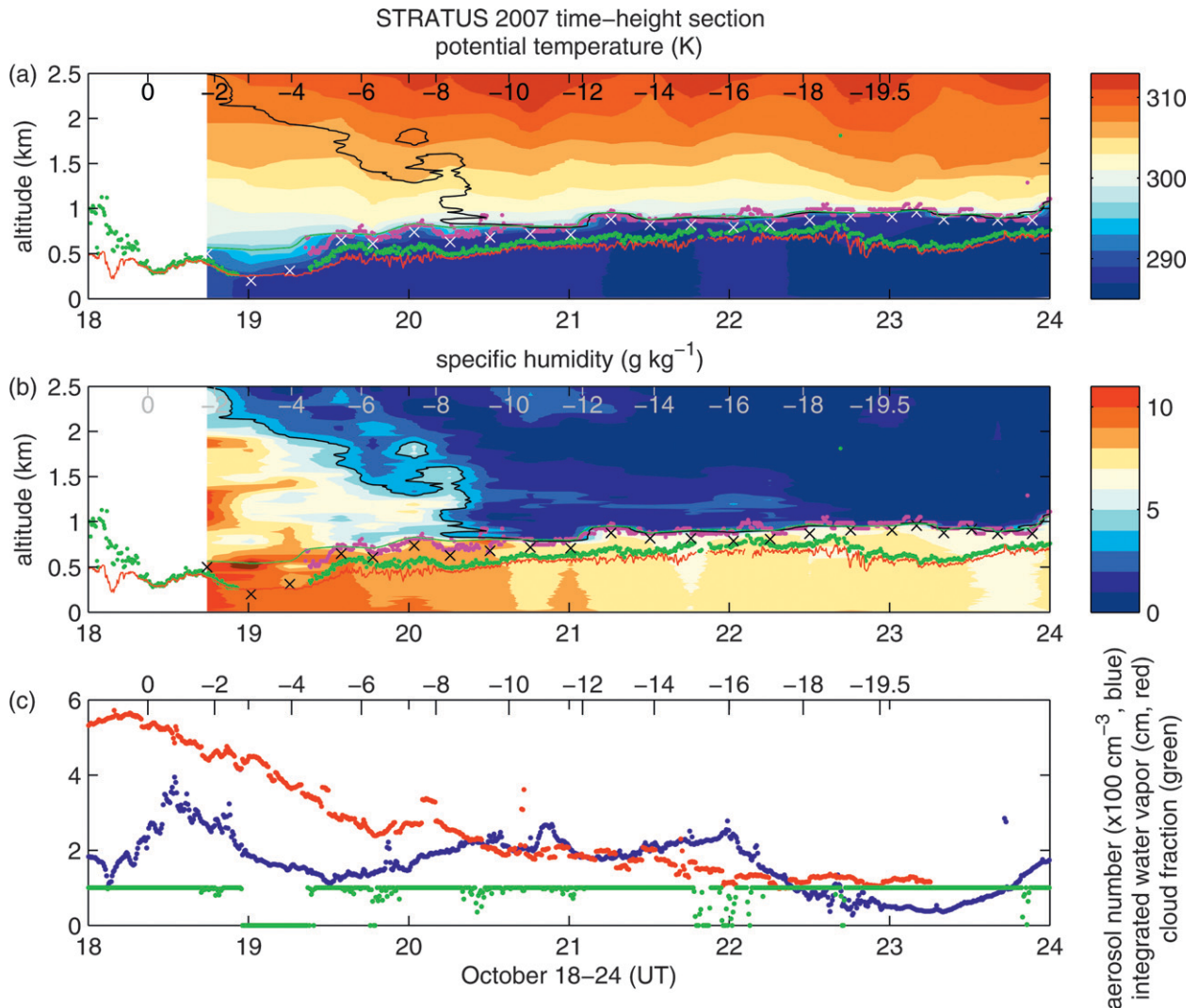
FIG. 2. Profiles of 0–2.5-km altitude lower-tropospheric (a) potential temperature and (b) specific humidity from rawinsondes. (c) Hundreds of aerosol particles per cubic centimeter (blue), column-integrated water vapor (cm, red), and cloud fraction (green). In (a) and (b) the crosses denote the height of minimum temperature at the base of the inversion. The green and black solid lines indicate the 296-K and 4 g kg^{-1} contours from the soundings, respectively. Green dots are the cloud base determined by the laser ceilometer, and magenta dots are the MABL inversion from the radar wind profiler. The red line is the lifting condensation level of a surface parcel. The horizontal coordinate is time, and the latitude of observation is printed along the top of each axis.

height section of potential temperature θ and specific humidity q from 0- to 2.5-km altitude in Figs. 2a,b. Both quantities clearly show the trade-MABL inversion after 20 October, with a well-mixed layer of high humidity (7–8 g kg^{-1}) and low potential temperature (287 K). By visual inspection we picked the 4 g kg^{-1} specific humidity (black) and 296-K (green) potential temperature contours to mark the boundary layer inversion. These contours follow the strong gradient at the MABL inversion south of 8°S, but the inversion is hard to diagnose north of 8°S. Before 20 October, the ship was under a convective weather system, with tall cumulus towers

reaching far into the free troposphere. The strong humidity signal of these clouds was recorded by the soundings. The 4 g kg^{-1} contour rises more than a kilometer into the free troposphere and the stratification of the inversion and free troposphere are reduced during this stormy period. The atmosphere remained convectively disturbed above 1 km all the way to 8°S, beyond the southern extent (2.5°S) of warm-pool SST over 20°C.

Apart from the convective period, marine atmospheric boundary layer stratocumulus clouds were quite uniform in height and thickness. We diagnose cloud top from the soundings, and compared them with other
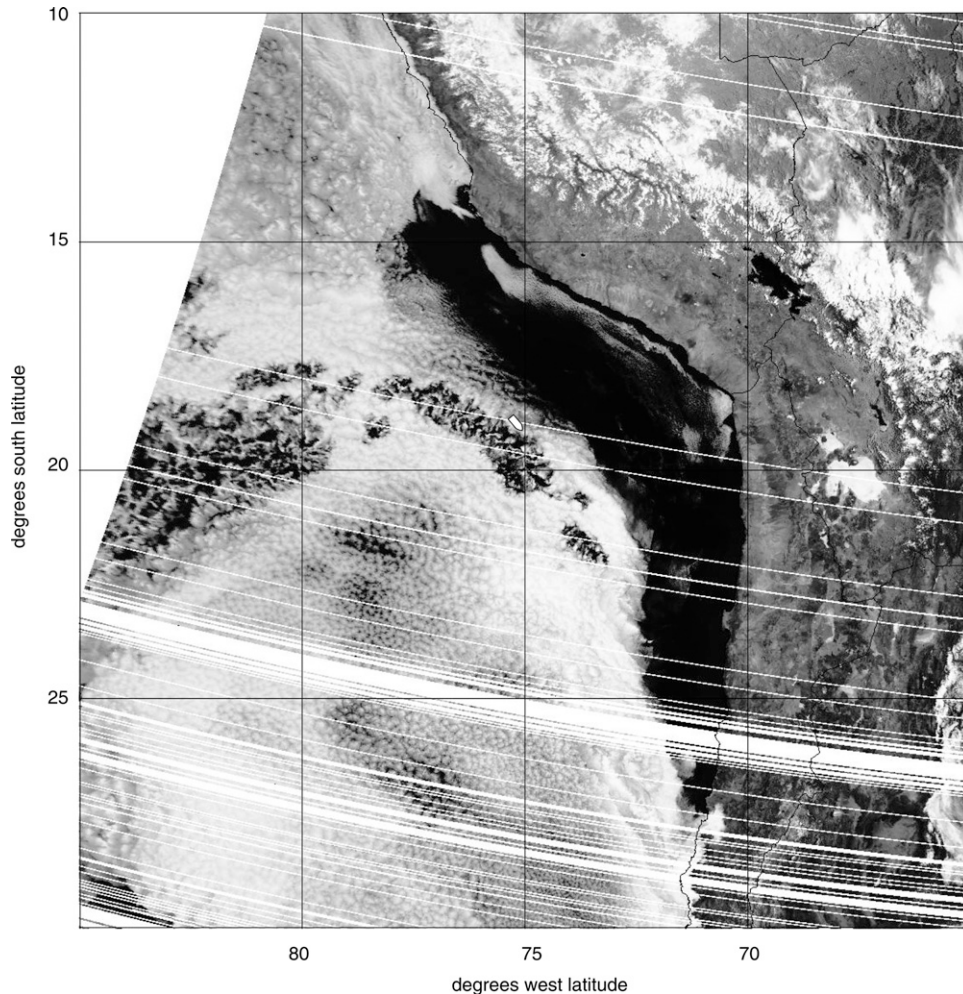
FIG. 3. Visible radiance from the *NOAA-17* polar-orbiting satellite on 1425 UTC 22 October. At the time of the image, the ship was at the position marked (18.6°S, 75.4°W) between the clear boundary layer neighboring the coast and the pocket of open cells to the southwest.

estimates from independent ship observations in Fig. 2a. (The estimates are repeated in Fig. 2b for comparison to the humidity profile.) The crosses show the height of the minimum temperature in the sounding, assumed to be the base of the inversion. The temperature minimum associated with cloud top is, on average, 100 m below the middle of the inversion indicated by strong gradients of humidity and potential temperature. The mean inversion base height is 800 ± 20 m for the coastal leg of the cruise. The NOAA PSD radar wind profiler receives strong signals scattered back from the gradients and turbulence at the inversion. Magenta dots show the height of maximum signal to noise ratio of the wind profiler radar returns. The wind profiler inversion height agrees well with the inversion found from the gradient in the soundings. These measures of the inversion height also correspond to the height where parcels

from the LCL would evaporate completely when mixed with 25%–50% of environmental air (not shown).

The stratocumulus cloud-base height observed by the laser ceilometer is plotted in green in Figs. 2a,b. The mean ceilometer cloud base is 640 m, and the mean LCL of a surface parcel is 570 m. The ceilometer cloud base is sometimes more than 100 m higher than the LCL of a surface parcel (red). This could be the result of dry air entrained from the free troposphere diluting the water vapor in the boundary layer or a subcloud layer in which humidity decreases with height (Caldwell et al. 2005). The consistency of cloud-base height from the ceilometer and the LCL and of the inversion height from the profiler and soundings gives us confidence in the accuracy of our measurements of cloud vertical structure.

The red line in Fig. 2c shows the integrated water vapor from the microwave radiometer. Integrated water

vapor follows the surface humidity (Fig. 1), as most of the water vapor is contained in the boundary layer. The clouds are usually solid, with cloud fraction (green, Fig. 2c) rarely deviating from unity. An exception is the clear sky observed in on the first half of 19 October (UTC), when the atmosphere is convective. Though partial clearing is observed on occasion, clear skies are only briefly observed in the stratocumulus region starting on the afternoons of 21–23 October (local time).

The concentration of aerosol particles between 0.1 and 5 μm is highest late on 18 October when the ship passes closest to land offshore of Cabo San Lorenzo. The aerosol concentration dips below 100 cm^{-3} on 22 October, with a minimum of 25 cm^{-3} on 23 October. Displacement of the ship further from shore on 22 October, after it had rounded Paracas Peninsula, could be responsible for the lower aerosol concentrations. Though clear skies were only observed briefly during these afternoons of lower aerosol concentration, the dip in aerosol concentration was similar to that in pockets of open cells (POCs; Stevens et al. 2005) observed during the remainder of the 2007 Stratus cruise.

The clearing seen from the ship in the early afternoon (local time) of 22 October was associated with a thickening of the cloud depth, with lower LCL and lower cloud base seen by the ceilometer in Fig. 2. Clouds remain thicker during the time of low aerosol concentrations. The visible-spectrum image from the *NOAA-17* polar-orbiting satellite taken on 1425 UTC 22 October (Fig. 3) corresponds to approximately 9 local time, and is the only satellite image from 22 October. The image in Fig. 3 shows two clear regions on either side of the ship, its position marked at the time of the image at 18.6°S, 75.4°W. The clear region adjoining the coast is most likely due to the boundary layer being too shallow for parcels to reach their LCL. The clear region neighboring the ship to its southwest is one of several POCs visible at this time. At the time of the image, the ship is barely outside the POC, but is headed south toward its wider end. On other days, progressions of several images throughout the day show POCs expanding into larger rifts of open cells during the afternoon.

5. Summary

In October 2007 the NOAA ship *Ronald H. Brown* followed the tropical Pacific coastline of western South America from the equator to 20°S. Surface ocean and meteorological measurements discern warm water near and displaced south of the equator and a cooler water mass south of 2.5°S. Winds blew parallel to the coast and were steady in speed and direction. Net heat gained by the surface of the ocean was 100 W m^{-2} over the

cool coastal water and not significantly different from zero over the warmer equatorial water.

Observations from multiple sensors were mutually consistent about the height of cloud bases and tops, and consistent with parcel and mixing-line computations of cloud vertical structure. Stratocumulus clouds were mostly solid, with only brief episodes of partial clearing, usually in the afternoon. Lower aerosol concentrations and slightly thicker clouds were observed 22–23 October when the ship encountered a pocket of open cells.

The data presented here are part of an integrated dataset (available at http://www.esrl.noaa.gov/psd/psd3/synthesis/). Sounding and in situ time series data are available for the Stratus cruises of 2001 and 2003–07. These data are suitable for verifying climatology, variability, and feedbacks in reanalysis and model products of the eastern tropical Pacific region. The various legs of these cruises also provide context for the VAMOS Ocean Cloud Atmosphere Land Study (VOCALS) Regional Experiment in autumn 2008, data from which are being collected and added to the integrated dataset as this article is going to press.

REFERENCES

Albrecht, B. A., C. S. Bretherton, D. Johnson, W. H. Schubert, and A. S. Frisch, 1995: The Atlantic Stratocumulus Transition Experiment—ASTEX. *Bull. Amer. Meteor. Soc.,* **76,** 889–904.

Bjerknes, J., 1969: Atmospheric teleconnections from the equatorial Pacific. *Mon. Wea. Rev.,* **97,** 163–172.

Caldwell, P., C. S. Bretherton, and R. Wood, 2005: Mixed-layer budget analysis of the diurnal cycle of entrainment in southeast Pacific stratocumulus. *J. Atmos. Sci.,* **62,** 3775–3791.

de Szoeke, S. P., and S.-P. Xie, 2008: The tropical eastern Pacific seasonal cycle: Assessment of errors and mechanisms in IPCC AR4 coupled ocean–atmosphere general circulation models. *J. Climate,* **21,** 2573–2590.

Fairall, C. W., and E. F. Bradely, 2006: A guide to making climate quality meteorological and flux measurements at sea. NOAA Tech. Memo. OAR PSD-311, NOAA Earth System Research Laboratory, Physical Sciences Division, 109 pp.

——, ——, J. E. Hare, A. A. Grachev, and J. B. Edson, 2003: Bulk parameterization of air–sea fluxes: Updates and verification for the COARE algorithm. *J. Climate,* **16,** 571–591.

——, T. Uttal, D. Hazen, J. Hare, M. F. Cronin, N. A. Bond, and D. E. Veron, 2008: Observations of cloud, radiation, and

surface forcing in the equatorial eastern Pacific. *J. Climate,* **21,** 655–673.

Garreaud, R. D., J. Rutllant, J. Quintana, J. Carrasco, and P. Minnis, 2001: CIMAR-5: A snapshot of the lower troposphere over the subtropical southeast pacific. *Bull. Amer. Meteor. Soc.,* **82,** 2193–2207.

Gordon, C. T., A. Rosati, and R. Gudgel, 2000: Tropical sensitivity of a coupled model to specified ISCCP low clouds. *J. Climate,* **13,** 2239–2260.

Ma, C.-C., C. R. Mechoso, A. W. Robertson, and A. Arakawa, 1996: Peruvian stratus clouds and the tropical Pacific circulation: A coupled ocean–atmosphere GCM study. *J. Climate,* **9,** 1635–1645.

Stevens, B., G. Vali, K. Comstock, R. Wood, M. C. V. Zanten, P. H. Austin, C. S. Bretherton, and D. H. Lenschow, 2005: Pockets of open cells and drizzle in marine stratocumulus. *Bull. Amer. Meteor. Soc.,* **86,** 51–57.

Xie, S.-P., 1994: On the genesis of the equatorial annual cycle. *J. Climate,* **7,** 2008–2013.

——, 2004: The shape of continents, air–sea interaction, and the rising branch of the Hadley circulation. *The Hadley Circulation: Past, Present and Future,* H. F. Diaz and R. S. Bradley, Eds., Kluwer Academic Publishers, 121–152.

Yuter, S. E., Y. L. Serra, and R. A. Houze Jr., 2000: The 1997 Pan American Climate Studies Tropical Eastern Pacific Process Study. Part II: Stratocumulus region. *Bull. Amer. Meteor. Soc.,* **81,** 483–490.

Zuidema, P., E. R. Westwater, C. Fairall, and D. Hazen, 2005: Ship-based liquid water path estimates in marine stratocumulus. *J. Geophys. Res.,* **110,** D20206, doi:10.1029/2005JD005833.